Fabrication of Flower-Like CoFe/C Composites Derived from Ferrocene-Based Metal-Organic Frameworks: An In-Situ Growth Strategy Toward High-Efficiency Electromagnetic Wave Absorption

*Xueling Wang, Xuan Zhang, Jiaqi Lu, and Zhiliang Liu**

Inner Mongolia Key Laboratory of Chemistry and Physics of Rare Earth Materials, College of Chemistry and Chemical Engineering, Inner Mongolia University, Hohhot 010021, P. R. China.

E-mail: cezlliu@imu.edu.cn, Fax: +86-471-4992922; Tel: +86-471-4992922

1. XRD Pattern and SEM images of Fc-based MOF

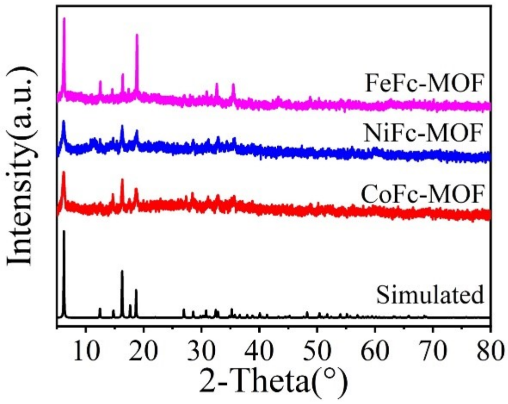

Figure S1 XRD pattern of Fc-based MOF.

The XRD pattern confirms that the obtained Fc-based MOF crystal structures are isostructural with those of the previously reported ZnFc-MOF.[1-3] Besides, in FeFc-MOF, the 2:3 M ratio of Fe^{3+}: Fe^{2+} made charge neutral.[4]

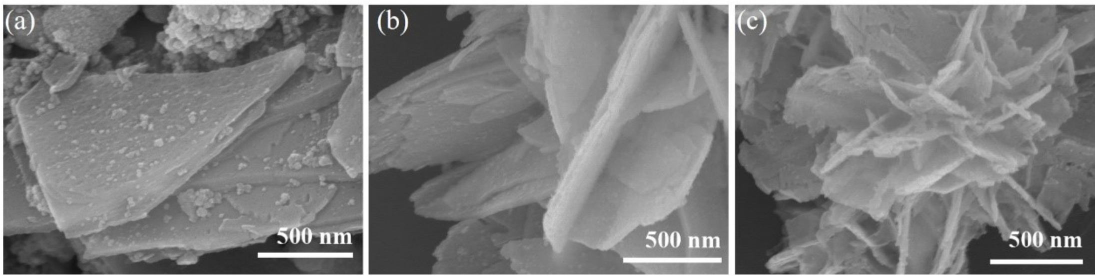

Figure S2 SEM images of precursors:(a) FeFc-MOF, (b) CoFc-MOF, (c) NiFc-MOF.

2. XPS Spectra

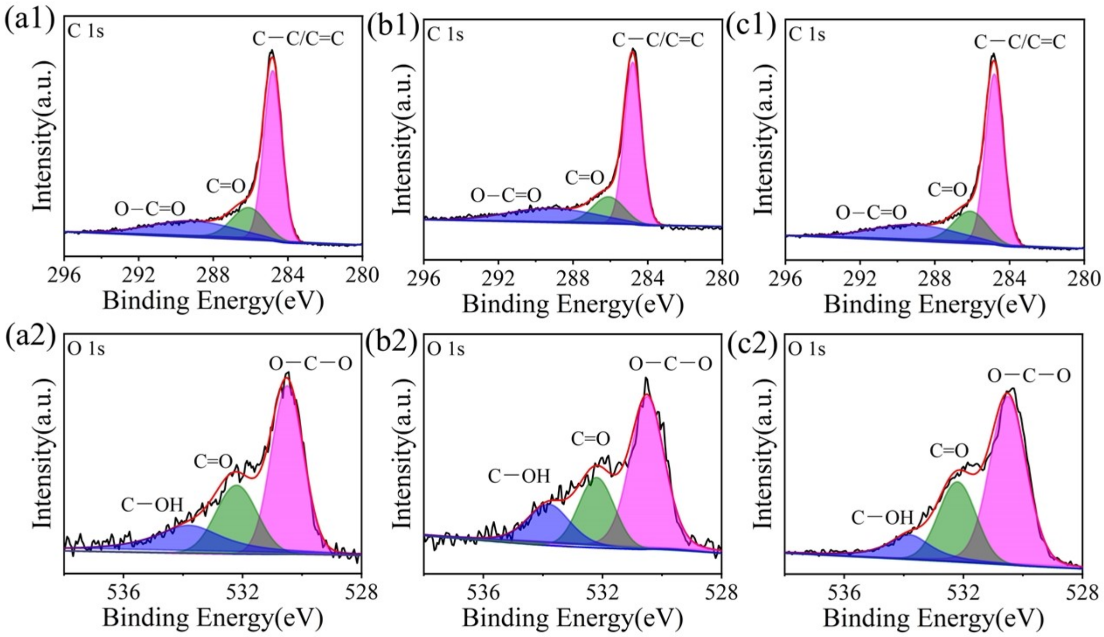

Fig. S3 High-resolution XPS of C 1s, and O 1s of (a) Fe/C, (b) CoFe/C, (c) NiFe/C.

3. Pore Size and Impedance Matching of MFe/C (M=Fe, Co, Ni)

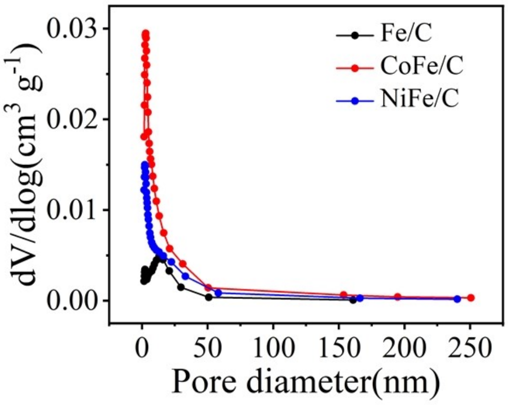

Fig. S4 Corresponding pore size distribution plots of the obtained composites.

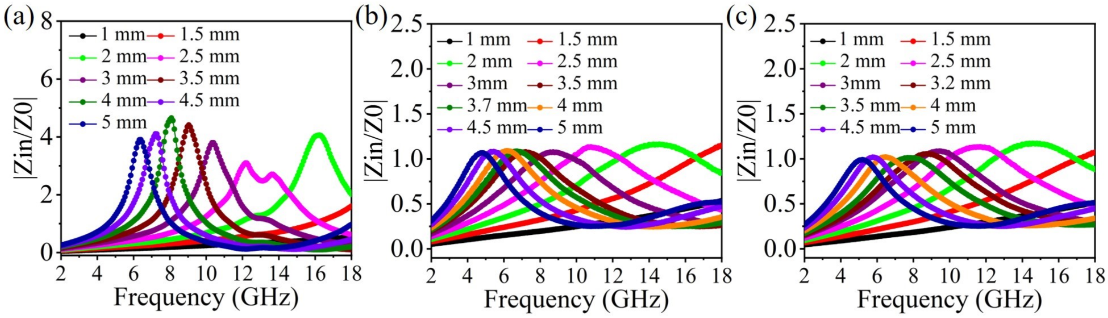

Fig. S5 The impedance matching values of (a) Fe/C, (b) CoFe/C, (c) NiFe/C.

4. Debey theory

In general, dielectric loss includes conduction loss and polarization relaxation, according to Debye theory, ε' and ε" can be expressed as follows: [5-8]

$$\varepsilon' = \varepsilon_\infty + \frac{\varepsilon_s - \varepsilon_\infty}{1+\omega^2\tau^2} \tag{1}$$

$$\varepsilon'' = \frac{(\varepsilon_s - \varepsilon_\infty)\omega\tau}{1+\omega^2\tau^2} + \frac{\sigma}{\omega\varepsilon_0} \tag{2}$$

$\boldsymbol{\varepsilon_s}$ and $\boldsymbol{\varepsilon_\infty}$ represent the static dielectric constant and the dielectric constant in the high-frequency limit, respectively, $\boldsymbol{\tau}$ is the relaxation time, $\boldsymbol{\omega}$ is the angular frequency of the electromagnetic wave, $\boldsymbol{\varepsilon_0}$ is the dielectric constant of free space, and $\boldsymbol{\sigma}$ is the conductivity. When σ is very low, $\sigma/\omega\sigma_0$ is negligible, so Equations (3) can be derived from the above two Equations:

$$\left(\varepsilon' - \frac{\varepsilon_s + \varepsilon_\infty}{2}\right)^2 + (\varepsilon'')^2 = \left(\frac{\varepsilon_s - \varepsilon_\infty}{2}\right)^2 \tag{3}$$

When ε' and ε'' satisfy equation (3), a semicircle in the ε'−ε" curve represents a Debye polarization relaxation process.[6]

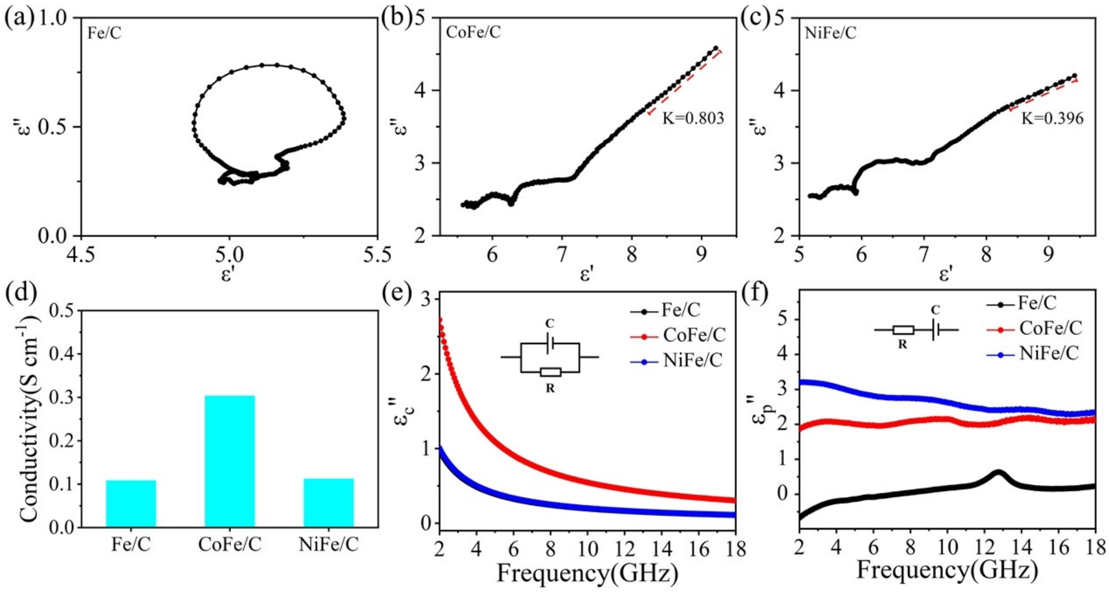

Fig. S6 (a−c) Cole−Cole curve of (a) Fe/C, (b) CoFe/C, (c) NiFe/C, (d) conductivity, (e) conduction loss, and (f) polarization loss of the obtained composites.

5. Quarter wavelength(1/4λ) matching model

The quarter wavelength(1/4λ) matching model is used to evaluate the correlation between matching thickness and reflection loss (RL) peak frequency, which can be expressed as follows: [9, 10]

$$t_m = \frac{\lambda}{4} = \frac{nc}{4f_m\sqrt{|\varepsilon_r \mu_r|}} \quad (n=1,3,5\ldots) \qquad (4)$$

$\boldsymbol{f_m}$ is the peak frequency, $\boldsymbol{\mu_r}$ is the relative complex permeability, $\boldsymbol{\varepsilon_r}$ is the relative complex permittivity, and ***c*** is the speed of light of electromagnetic waves in free space.

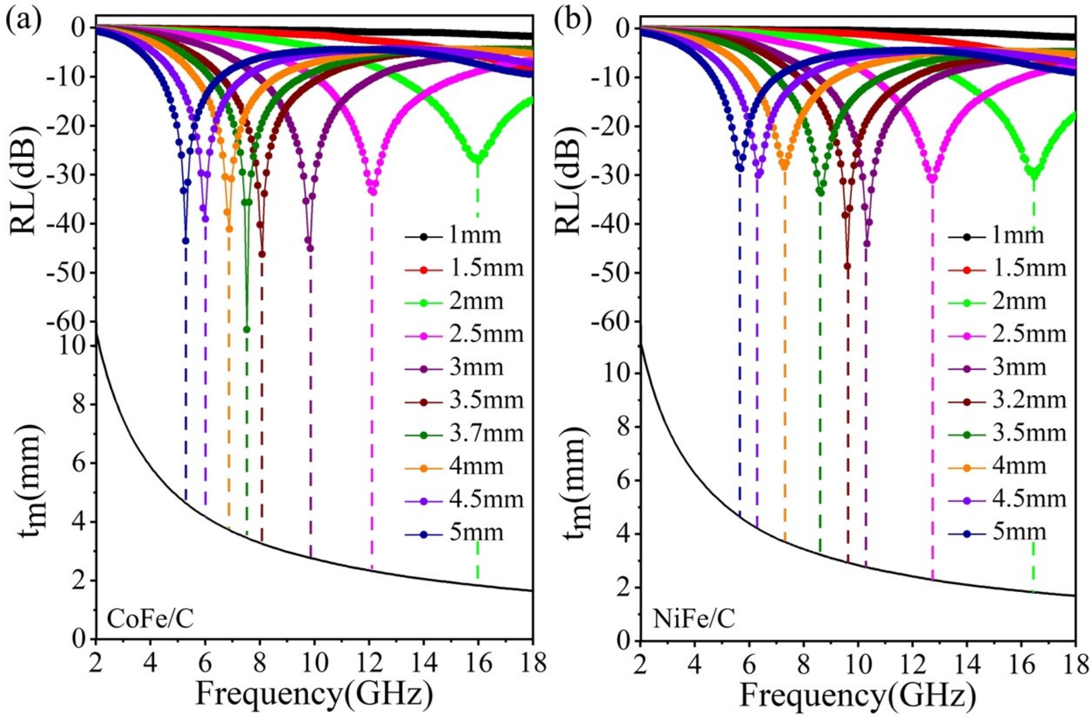

Fig. S7 Dependence of reflection loss on quarter-wavelength of (a) CoFe/C, (b) NiFe/C.

6. Radar cross-section (RCS) simulation

Radar cross section (RCS) is the most critical physical indicator in radar stealth technology, which is used to evaluate the military value of materials.[11-13] The RCS value was calculated as follows: [13]

$$RCS(dBm^2 = 10\log\left(\frac{4\pi S}{\lambda^2}\left|{E_S}/{E_i}\right|\right) \tag{5}$$

S represents the area of the model, ***λ*** denotes the wavelength of the EMW, $\boldsymbol{E_s}$ and $\boldsymbol{E_i}$ stand for the electric field intensity of the incident and scattered waves, respectively.

References

1. D. Guo, H. Mo, C. Duan, L. Feng and Q. Meng, *J. Chem. Soc., Dalton Trans.*, 2002, 2593-2594.
2. J. Huo, L. Wang, E. Irran, H. Yu, J. Gao, D. Fan, B. Li, J. Wang, W. Ding, A. M. Amin, C. Li and L. Ma, *Angew. Chem. Int. Ed.*, 2010, **49**, 9237-9241.
3. J. Liang, X. Gao, B. Guo, Y. Ding, J. Yan, Z. Guo, E. C. M. Tse and J. Liu, *Angew. Chem. Int. Ed.*, 2021, **60**, 12770-12774.
4. C. Li, C. Zhang, J. Xie, K. Wang, J. Li and Q. Zhang, *Chem. Eng. J.*, 2021, **404**, 126463.
5. L. Gai, Y. Zhao, G. Song, Q. An, Z. Xiao, S. Zhai and Z. Li, *Compos. Part A-appl. S.*, 2020, **136**, 105965.
6. Y. Zhang, X. Liu, Z. Guo, C. Jia, F. Lu, Z. Jia and G. Wu, *J. Mater. Sci. Technol.*, 2024, **176**, 167-175.
7. C. Wang, H. Jiang, B. Cui, X. Xu, M. Li, Z. Xu, H. Tan, D. Yang, Y. Feng, Y. Wang and C. Wang, *Chem. Eng. J.*, 2023, **475**, 146298.
8. Y. Guo, Y. Duan, X. Liu, H. Zhang, T. Yuan, N. Wen, C. Li, H. Pan, Z. Fan and L. Pan, *Small*, 2023, 2308809.
9. Y. Ma, Y. Jiang, J. Qian, C. Wang, S. Kang, G. Chen and B. Zhong, *Ceram. Int.*, 2023, **49**, 18745-18755.
10. Z. Qin, C. Wang, Y. Ma, L. xia, B. Zhong, X. Li and P. Zhang, *Appl. Surf. Sci.*, 2022, **575**, 151789.
11. F. Zhang, N. Li, J.-F. Shi, Y.-Y. Wang, D.-X. Yan and Z.-M. Li, *Small*, 2024, 2312135.
12. W. Deng, T. Li, H. Li, J. abdul, L. Liu, A. Dang, X. Liu, M. Duan and H. Wu, *Small*, 2024, 2309806.
13. L. Xing, H. Cheng, Y. Li, Q. Chen and X. Liu, *Chem. Eng. J.*, 2024, **487**, 150729.